The typhoon wind hazard assessment considering the correlation among the key random variables using the Copula method

Xu Hong

School of Civil Engineering, Hefei University of Technology, 193 Tunxi Road, Heifei, 230009, China

Anhui Key Laboratory of Civil Engineering Structures and Materials, 193 Tunxi Road, Heifei, 230009, China

Email: xhong@hfut.edu.cn

Yupeng Song

College of Civil Engineering, Nanjing Tech University, 30 Puzhu Road(S), Nanjing, 211816, China

Email: songyupeng@njtech.edu.cn (Corresponding author)

Fan Kong

School of Civil Engineering, Hefei University of Technology, 193 Tunxi Road, Heifei, 230009, China

Anhui Key Laboratory of Civil Engineering Structures and Materials, 193 Tunxi Road, Heifei, 230009, China

Email: kongfan@hfut.edu.cn

Michael Beer

Institute for Risk and Reliability, Leibniz Universität Hannover, Callinstr 34, 30167 Hanover, 30167, Germany

Institute for Risk and Reliability, University of Liverpool, Peach Street, Liverpool, L69 7ZF, UK

International Joint Research Center for Resilient Infrastructure & International Joint Research Center for Engineering Reliability and Stochastic Mechanics, Tongji University, Shanghai, 200092, China

Email: beer@irz.uni-hannover.de

Abstract: The probability distribution of typhoon key parameters is commonly incorporated with typhoon models to estimate the typhoon-induced wind speeds associated with certain return periods in the typhoon-prone region. In most studies that focus on the typhoon wind hazards of the southeast coastline of China, the typhoon key parameters are assumed to be independent. This paper develops a Copula-based joint probability distribution for the typhoon key parameters to investigate its potential influence on the typhoon wind hazard on the southeast coastline of China. To this end, the best track typhoon data from the China meteorological administration is used to extract the key parameters of the typhoon. The analyses show that the observed correlation coefficients among the parameters could be larger than 0.4 at some locations on the considered coastline. The C-vine copula is then employed to establish the joint probabilistic model of these key parameters. Comparison between the observed and modeled joint probability distributions suggests the adequacy of the Copula method based probability distribution model. Then a local track model and a typhoon wind field model are assembled to simulate the history of the typhoon-induced surface wind given the typhoon key parameters. Finally, Monte Carlo simulation is adopted to estimate the wind speed associated with 50- and 100-year return periods. Results show that neglecting the correlation among the typhoon key parameters could cause a relative difference of up to 7% at some locations on the coastline.

Keywords: Typhoon, joint probability distribution, Copula method, wind hazard, correlation.

Introduction

A typhoon, also known as a tropical cyclone or hurricane, is one of the great natural disasters associated with strong winds, heavy rain, storm surges, and tornadoes. The western North Pacific (WNP) is the most active basin for typhoons on the planet, with one-third of all typhoon activity. The southeast coast of China, located in the WNP, suffers greatly from typhoon disasters with more than six typhoons making landfall on its coastline every year. It is reported that in mainland China an average annual direct economic loss of 69.5 billion RMB was caused by typhoons from 2005 to 2016, accounting for more than 1% of the annual gross domestic product (Wang et al., 2019). Most economic losses can be attributed to structure destruction or function failure. To both ensure the safety of engineering structures and enhance the resilience of coastal communities, it is desired to evaluate the extreme wind hazard associated with the typhoon disaster (Lu et al., 2022; Khajwal and Noshadravan, 2020).

Evaluating the wind hazard in regions where the well-behaved weather system governs the local climate usually involves fitting the observed histogram of the annual maximum surface winds to a probability distribution (Hu et al., 2023). However, reliable observations of typhoon surface winds are very limited because the occurrence rate of typhoons at a specific site is rare and also because the anemometers usually are non-functional and even damaged during devastating typhoon disasters (Fang et al., 2020). Due to the paucity of observations, the statistical fitting approach is not applicable in assessing the typhoon wind hazard in typhoon-prone regions. Alternatively, the typhoon hazard assessment based on artificially generating the typhoon surface wind scenarios has been developed since the pioneering works by Russell (1971) and Batts et al. (1980). In this approach, models are used to generate the typhoon surface winds with the input of the meteorological variables of which the observations are relatively sufficient, such as the typhoon central pressure deficit. With the help of the randomly sampled meteorological variables and the Monte Carlo simulation technique, a set of artificial typhoon surface wind scenarios can be obtained, and the wind speeds associated with specific return periods can be estimated. The typhoon hazard assessment basically consists of two components, i.e., a typhoon track model and a typhoon wind field model. The typhoon track models can be classified into full track models and local track models. A full track model is capable of representing the whole track during the typhoon's lifetime (Chen and Duan, 2018; Emanuel et al., 2006; Hong and Li, 2021; Vickery et al., 2000), while the local track model is aimed at representing the segment of the typhoon track that is adjacent to the considered site with a straight line (Georgiou et al., 1983; Hong et al., 2016; Vickery and Twisdale, 1995). This study mainly focuses on the local track approach because it is sufficient in many engineering applications where only the specific site is considered.

In the local track approach, the typhoon key parameters determining the surface winds typically include the central pressure deficit (Δp), minimum distance from the site of interest to the typhoon center ($D_{\min}$), translational velocity (U_t), heading (θ), radius of maximum wind ($\underline{R}_{\max}$), and shape parameter of the pressure profile (B). As shown in Figure 1, the typhoon track can be fully described by $D_{\min}$, U_t, and θ. $D_{\min}$ is positive if the site is on the right side of the typhoon translation direction. θ is the angle rotating from the true north to the typhoon heading clockwise. Then, Δp, $\underline{R}_{\max}$ and B are used to calculate the surface wind history with the help of a wind field model (Fang et al., 2018a; Hong et al., 2019; Kepert and Wang, 2001; Li and Hong, 2015a; Thompson and Cardone, 1996) when the typhoon is moving along the local track. In essence, the typhoon models form a mapping from the probability space of typhoon key parameters to that of surface wind. Thus, modeling the probability distributions of the typhoon key parameters is vital in the typhoon hazard assessment, and great efforts have been made to improve the fidelity of their probability distribution models. To avoid the unrealistically high values of Δp, Batts et al. (1980) used a censored lognormal distribution for Δp. Georgiou (1985) examined the most suitable probability distribution for the typhoon key parameters from several candidate distributions by statistical tests. Vickery et al. (1995) examined the von Mises distribution, normal distribution, and binormal distribution for θ, and they found that the heading of a typhoon is best modeled using a binormal distribution. The AIC criterion was adopted by Li and Hong (2015b) to select the best-fit distributions. Also, the Anderson-Darling distance was used by Hong and Li (2022) in determining the distribution of Δp for its capability of distinguishing the difference of the tail part of Δp to which the wind hazard is largely sensitive. It is worth pointing out that extensive efforts (Georgiou, 1985; Vickery and Twisdale, 1995; Vickery and Wadhera, 2008; Xiao et al., 2011) have been made to develop the statistical models relating R_{max} and B to other typhoon key parameters, such as Δp.

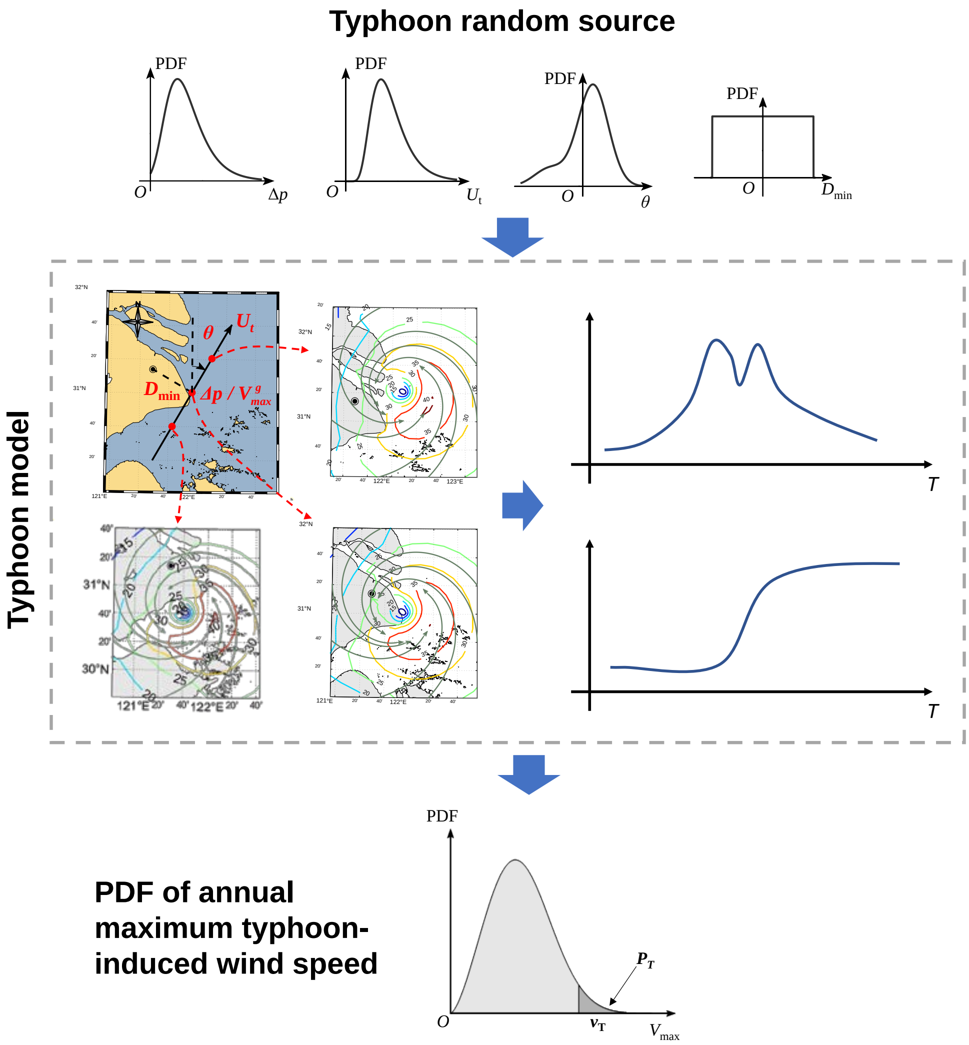

Figure 1 Illustration of typhoon hazard assessment.

Compared with these well-developed statistical correlation models of R_{max} and B to other parameters, the literature review indicates that studies on the correlation among D_{min}, U_t, θ and Δp are relatively limited. Vickery and Twisdale (1995) is one of the earliest studies considering the dependence of Δp and U_t on θ. They modeled both the logarithmic mean of U_t and scale parameter in the Weibull distribution for Δp as linear functions of θ. This approach could be inconvenient when the correlation among all parameters is desired to be considered simultaneously. To address this problem, Ishihara et al. (2005) proposed a modified orthogonal decomposition method to model the random vector comprised of the key typhoon parameters to be a linear transform from independent random variables. Nevertheless, as the orthogonal decomposition method is based on the correlation matrix of the random vector, it can only reproduce the second-order statistics and might not capture the higher-order information. Wu et al. (2021) obtained the joint distribution model of the key typhoon parameters by incorporating the Nataf transform. However, a Gaussian dependence structure of the random variables is assumed in this method, which may not reflect the true situation. Recently, the use of copula method in modeling the correlations between random variables has received more and more attention in various engineering applications (Nelsen, 2006; Song et al., 2022; Tang et al., 2015; Tao et al., 2020; Jäger and Nápoles, 2017; Candela and Aronica, 2017). In this method, the marginal distribution of variables and the dependence structure can be addressed separately, and various types of copulas have been developed to describe the dependence characteristics. Therefore, this method has shown remarkable advantages over other correlation modeling techniques in terms of accuracy and flexibility (Song et al., 2021). Given this, it is desired to incorporate the copula method in typhoon hazard analysis to improve the fidelity of modeling joint probability distribution for the typhoon key parameters. Moreover, though the influence of the correlations among typhoon key parameters on the typhoon hazard has been investigated for several cities (Wu et al., 2021), a similar study for the whole coastline is unavailable in the literature to the best of the authors' knowledge.

To conclude, this study aims to investigate the influence of the correlations of the typhoon key parameters on the typhoon wind hazard at the southeast coastline of China using the copula method. The methodology of the Copula method, the data used in the study, and modeled probability distribution for typhoon key parameters is first presented; then the procedure of assessing the typhoon wind hazard is illustrated; next, the analyzed results of the influence of the correlation among the typhoon key parameters on the typhoon wind hazards is presented.

Modeling the probability distribution for typhoon key parameters

Copula method

The C-vine copula developed specifically for modeling multiple random variables is adopted in the present study to model the joint distribution of the typhoon key parameters. Although details on this method can be found in the literature (Aas et al., 2009; Song et al., 2021; Tao et al., 2020), the basic principles of the method are briefly interpreted herein for easy understanding. For clarity, consider a four-dimensional random vector $\left(X_1, X_2, X_3, X_4\right)^{\mathrm{T}}$, and the joint probability density function (PDF) is expressed in the configuration of C-vine copula as (Aas et al., 2009)

$$\begin{aligned} f\left(x_1, x_2, x_3, x_4\right) = & f_1 f_2 f_3 f_4 c_{12}\left(F_1, F_2\right) c_{13}\left(F_1, F_3\right) c_{14}\left(F_1, F_4\right) \\ & \cdot c_{23|1}\left(F_{2|1}, F_{3|1}\right) c_{24|1}\left(F_{2|1}, F_{4|1}\right) c_{34|12}\left(F_{3|12}, F_{4|12}\right), \end{aligned} \tag{1}$$

where $f_i = f_{X_i}\left(x_i\right)$ and $F_i = F_{X_i}\left(x_i\right)$ denote the marginal PDF and the cumulative distribution function (CDF) of $X_i \left(i = 1, 2, 3, 4\right)$, respectively; $\left\{F_{i|1}, i = 2, 3, 4\right\}$ and $\left\{F_{i|12}, i = 3, 4\right\}$ are the conditional marginal CDFs; $\left\{c_{1i}\left(\cdot, \cdot\right), i = 2, 3, 4\right\}$, $\left\{c_{2i|1}\left(\cdot, \cdot\right), i = 3, 4\right\}$ and $c_{34|12}\left(\cdot, \cdot\right)$ denote the bivariate copula density functions.

It is seen in Eq.(1) that the joint PDF of a multivariate is expressed as the product of the marginal PDFs of variables and the dependence structure represented by a series of bivariate copula density functions. The bivariate copula density function $c\left(u, v; \lambda\right)$ is defined as

$$c\left(u, v; \lambda\right) = \frac{\partial^2 C\left(u, v; \lambda\right)}{\partial u \partial v}, \tag{2}$$

where $u = F_X\left(x\right)$ and $v = F_Y\left(y\right)$ are the CDFs of the variables X and Y, respectively; $C\left(\cdot, \cdot\right)$ denotes the bivariate copula function; and λ is the parameter of the copula.

To facilitate understanding, the tree-like structure can be used to describe the C-vine copula configuration (Aas et al., 2009), and is shown in Figure 2 for the four-dimensional random vector. It is seen that the dependence structure is comprised of three trees, each with a local dominant random variable connected to the other variables through bivariate copulas. The order of the variable dominating the whole dependence structure is determined by the degree of correlation of the variable with the other variables (Dißmann et al., 2013; Song et al., 2021). For instance, in Figure 2, the dominant and subdominant variables of the dependence structure are X_1 and X_2, respectively. Once the dominating order of the variables and the associated bivariate copulas are determined, the dependence structure can be readily obtained.

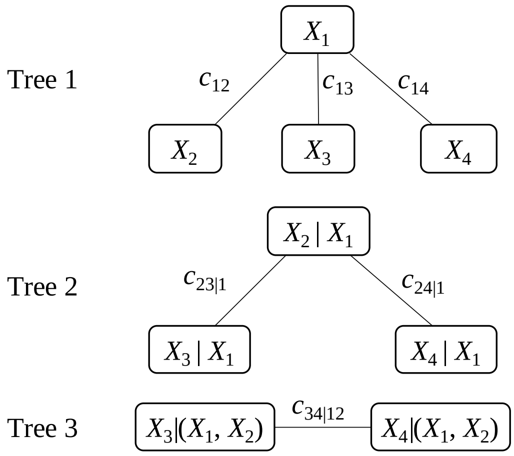

Figure 2 The tree-like structure of C-vine copula in the four-dimensional case.

Various bivariate copulas are available in the literature, and the elliptical and Archimedean copula families are widely used in practice (Nelsen, 2006). The elliptical copula family mainly includes the Gaussian copula and Student's t copula, and the Archimedean copula family mainly includes the Frank copula, Gumbel copula, and Clayton copula. Each bivariate copula defines a specific dependence structure for a pair of random variables. Several widely used copulas are shown in Table 1. In this table, $t_{\lambda,\chi}\left(\cdot,\cdot\right)$ denotes the bivariate standard Student's t distribution with the degrees of freedom χ and the correlation coefficient λ, and $t_{\chi}^{-1}\left(\cdot\right)$ is the inverse of the standard Student's t distribution with the degree of freedom χ ; $\Phi_{\lambda}\left(\cdot,\cdot\right)$ represents the bivariate standard Gaussian distribution with the correlation coefficient λ, and $\Phi^{-1}\left(\cdot\right)$ is the inverse of the standard Gaussian distribution.

Table 1 Bivariate copulas (Song et al., 2022)

Copula type	Copula function $C(u, v; \lambda)$	Range of λ
Student's t	$t_{\lambda,\chi}\left(t_\chi^{-1}(u), t_\chi^{-1}(v)\right)$	$[-1, 1]$
Gaussian	$\Phi_\lambda\left(\Phi^{-1}(u), \Phi^{-1}(v)\right)$	$[-1, 1]$
Frank	$-\ln\left[1+\left(e^{-\lambda u}-1\right)\left(e^{-\lambda v}-1\right)/\left(e^{-\lambda}-1\right)\right]/\lambda$	$(-\infty, 0)\cup(0, +\infty)$
Clayton	$\left(u^{-\lambda}+v^{-\lambda}-1\right)^{-1/\lambda}$	$(0, +\infty)$
Gumbel	$\exp\left\{-\left[(-\ln u)^\lambda+(-\ln v)^\lambda\right]^{1/\lambda}\right\}$	$[1, +\infty)$

The rotation versions of the above copulas are usually adopted in practice as well to describe the negative dependence between pairs of variables (Song et al., 2022). It is worth pointing out that the copulas mentioned above are all symmetric copulas, which are not capable of representing the asymmetric dependence characteristics between variables. To address this issue, several different methods for constructing asymmetric copulas were proposed, and one of the most widely used forms is expressed as (Fazeres-Ferradosa et al., 2018)

$$\tilde{C}(u, v; \lambda) = C\left(u^\alpha, v^\beta; \lambda\right)\cdot u^{1-\alpha}v^{1-\beta}, \tag{3}$$

where $C(\cdot,\cdot)$ denotes the ordinary symmetric copula; and $\alpha, \beta\ (0\le\alpha,\beta\le1)$ are the parameters to be determined.

It should be noted that the heading (θ), which is a circular variable, is involved in the joint probabilistic modeling of typhoon key parameters. The circular variable is defined on the unit circle with a cycle period of 2π radians, distinguishing it from the linear variables such as the translational velocity. Therefore, dedicated copulas should be adopted to model the dependence structure between circular and linear variables. Currently, the QS copula (García-Portugués et al., 2013) and the JW copula (Johnson and Wehrly, 1978) are usually employed for this problem. The QS copula has the following formula,

$$C(u, v; \lambda) = uv + \lambda\sin(2\pi u)v(1-v), \tag{4}$$

where $u = F_{\Theta}(\theta)$ and $v = F_X(x)$ are the CDFs of the circular and linear variables, respectively; and λ denotes the copula parameter, $|\lambda| \le 1/(2\pi)$.

The maximum likelihood estimation method can be adopted to determine the copula parameters, and the optimal copula can be selected from the model candidates according to some criteria. Besides, the goodness-of-fit test should be carried out to judge whether the obtained copula can well represent the dependence structure of the random variables. Details on the parameter estimation, the goodness-of-fit test, and the optimal model selection are not elaborated herein to avoid lengthiness and can be referred to Refs. (Aas et al., 2009; Tao et al., 2020).

According to Eq.(1), to obtain the joint PDF of the typhoon key parameters, the marginal distributions and the dependence structure should be respectively estimated, which are addressed in the next two subsections.

Marginal probability distributions of typhoon key parameters

To model the marginal probability distributions of the typhoon key parameters, the observed samples of Δp, $D_{\min}$, U_t and θ are extracted from the best-track dataset from the CMA (Lu et al., 2021). The CMA best-track dataset contains information on the typhoon center latitude, longitude, and minimum sea level pressure of the historical typhoons in WNP every six hours. The data of historical typhoons from 1980 to 2013 is used in this study. It should be noted that the probabilistic characteristics are not necessarily time-invariant because of the change of climate (Lombardo and Ayyub, 2017). As this study is focused on the correlations between the typhoon key parameters and their influence on the typhoon wind hazard, the climate change issue will not be considered. In the data processing, a circular region centered at the site of interest with a radius of 250 km is defined, and only typhoons entering the circular regions are regarded to contribute to the ensemble of typhoon key parameters. Despite the ROCI (radius of outermost closed isobar) is typically around 500 km or even larger, the extreme wind speed in typhoons usually occurs at a smaller radius. Yuan et al. (2007) showed that the radius of 25.7 m/s winds for typhoons on the Chinese southeast coast is mostly less than 250 km. Note that the 50-year return period value of the 10-min mean speed at the surface in the considered coastal region is generally higher than 30 m/s, it is believed the circular radius of 250 km is adequate to capture the extreme wind in the typhoon. For $D_{\min}$, U_{t}, and θ, values at the position closest to the interested site are used as the observed samples; for Δp, the value when the typhoon is first entering the circular region is used for the minimum sea level pressure, and then an ambient pressure of 1010 hPa is adopted to calculate Δp.

Following Georgiou (1985), Xiao et al. (2011), and Li and Hong (2015b), to select the most suitable probability distribution for the typhoon key parameters, several candidate probability distribution models are considered. For both U_{t} and Δp, the candidate probability distributions are the lognormal, gamma, Gumbel, or Weibull distributions; $D_{\min}$ can be modeled as trapezoidal, uniform, and quadratic distribution; and θ is modeled as the binormal distribution. Following Hong and Li (2022), the maximum likelihood estimation is used to determine the parameters of the candidate probability distribution, and in selecting the most suitable probability distribution the AIC criterion is utilized for U_{t} and $D_{\min}$, and the Anderson–Darling distance is used for Δp.

For convenience, the kilometer post of the southeast coastline of China and nine key cities on the coastline are shown in Figure 3. The most suitable probability distributions for the typhoon key parameters at the considered cities are shown in Table 2, and the probability distribution models used in this study are tabulated in Table 3.

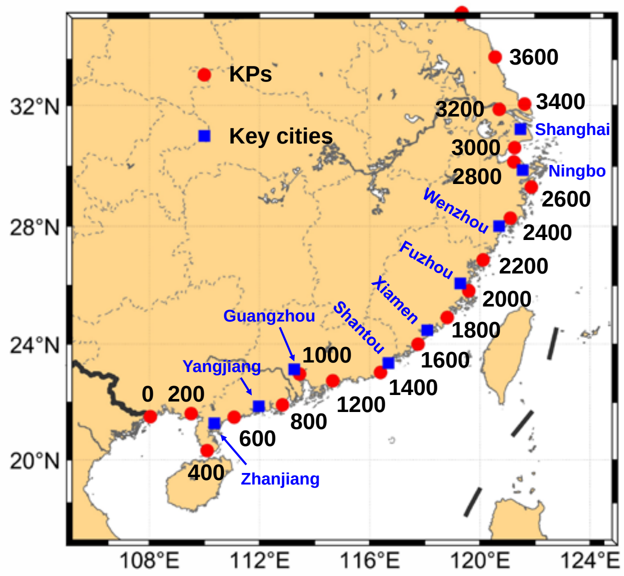

Figure 3 Definition of the kilometer post and the location of considered key cities.

Table 2 Probability distributions for the typhoon key parameters.

City	U_t	$D_{\min}$	ϑ_t	Δp	ξ
Shanghai	Gumbel μ = 6.26 m/s, σ = 2.63 m/s	Uniform a = -250 km, b = 250 km	Binormal t = 0.08, μ_1 = 1.11 rad, σ_1 = 0.05 rad, μ_2 = -0.075 rad, σ_2 = 0.76 rad	Weibull μ = 25.15, σ = 1.64 hPa	1.38
Ningbo	Log normal μ = 1.93 m/s, σ = 0.42 m/s	Uniform a = -250 km, b = 250 km	Binormal t = 0.63, μ_1 = 0.35 rad, σ_1 = 0.49 rad, μ_2 = -0.75 rad, σ_2 = 0.53 rad	Weibull μ = 31.9, σ = 1.69 hPa	1.59
Wenzhou	Gamma a = 5.45, b = 1.25 m/s	Uniform a = -250 km, b = 250 km	Binormal t = 0.46, μ_1 = 0.46 rad, σ_1 = 0.32 rad, μ_2 = -0.98 rad, σ_2 = 0.52 rad	Weibull μ = 35.3, σ = 1.75 hPa	1.86
Fuzhou	Gumbel μ = 4.63 m/s, σ = 2.33 m/s	Uniform a = -250 km, b = 250 km	Binormal t = 0.09, μ_1 = 1.18 rad, σ_1 = 0.20 rad, μ_2 = -0.71 rad, σ_2 = 0.65 rad	Weibull μ = 39.56, σ = 2.18 hPa	2.41
Xiamen	Gumbel μ = 4.58 m/s, σ = 2.14 m/s	Uniform a = -250 km, b = 250 km	Binormal t = 0.81, μ_1 = -0.56 rad, σ_1 = 1.06 rad, μ_2 = -1.22 rad, σ_2 = 0.09 rad	Weibull μ = 36.35, σ = 2.01 hPa	2.57
Shantou	Weibull μ = 6.1, σ = 2.59 m/s	Uniform a = -250 km, b = 250 km	Binormal t = 0.59, μ_1 = -0.04 rad, σ_1 = 0.90 rad, μ_2 = -1.29 rad, σ_2 = 0.40 rad	Lognormal μ = 3.23, σ = 0.60	2.68
Guangzhou	Gumbel μ = 4.46, σ = 2.15 m/s	Trapezoidal a = -250 km, b = 250 km, t = 0.34	Binormal t = 0.072, μ_1 = 1.28 rad, σ_1 = 0.11 rad, μ_2 = -0.82 rad, σ_2 = 0.71 rad	Gumbel μ = 20.17 hPa, σ = 12.20 hPa	2..54
Yangjiang	Weibull μ = 6.17, σ = 2.53 m/s	Uniform a = -250 km, b = 250 km	Binormal t = 0.53, μ_1 = -0.61 rad, σ_1 = 1.02 rad, μ_2 = -1.14 rad, σ_2 = 0.28 rad	Gumbel μ = 19.35 hPa, σ = 12.40 hPa	3.16
Zhanjiang	Weibull μ = 5.95, σ = 2.88 m/s	Trapezoidal a = -250 km, b = 250 km, t = 0.33	Binormal t = 0.50, μ_1 = -0.35 rad, σ_1 = 1.41 rad, μ_2 = -1.27 rad, σ_2 = 0.34 rad	Lognormal μ = 3.10, σ = 0.65	3.32

Table 3 Probability distribution model used in this study.

Distribution type	Probability density function
Lognormal	$p(x)=\frac{1}{x\sigma\sqrt{2\pi}}\exp\left[-\frac{1}{2}\left(\frac{\ln x-\mu}{\sigma}\right)^2\right], x>0$, where μ and σ are the mean value and standard deviation of the variable's natural logarithm.
Gumbel	$p(x)=\exp\left\{-\exp\left[-\frac{x-\mu}{\sigma}\right]\right\}$, where μ is the location parameter and σ is scale parameters.
Gamma	$p(x)=\frac{1}{b^a\Gamma(a)}x^{a-1}\mathrm{e}^{-\frac{x}{b}}$, where a is the shape parameter and b is scale parameters, and $\Gamma(\cdot)$ is the Gamma function.
Weibull	$p(x)=\frac{\mu}{\sigma}\left(\frac{x}{\sigma}\right)^{\mu-1}\exp\left[-\left(\frac{x}{\sigma}\right)^{\mu}\right], x>0$, where μ is the shape parameter and σ is the scale parameter.

Uniform	$p(x)=\frac{1}{b-a}, x\in[a,b]$, where a and b are model parameters.
Trapezoidal	$p(x)=\frac{1}{b-a}+t\left(x-\frac{a+b}{2}\right), x\in[a,b]$, where a, b and t are model parameters.
Binormal	$p(x)=\frac{t}{\sigma_1\sqrt{2\pi}}\exp\left[-\frac{1}{2}\left(\frac{x-\mu_1}{\sigma_1}\right)^2\right]+\frac{1-t}{\sigma_2\sqrt{2\pi}}\exp\left[-\frac{1}{2}\left(\frac{x-\mu_2}{\sigma_2}\right)^2\right]$, where t is the combination parameter, μ_1 and σ_1 are the mean and standard deviation for the first mode, and μ_2 and σ_2 are the mean and standard deviation for the second mode.

Dependence structure of typhoon key parameters

Before the joint probability distributions for typhoon key parameters are modeled using the Copula method, the correlations among these parameters are investigated. The variation of the correlation coefficients with the kilometer post is displayed in Figure 4, where several observations can be made. First, the correlations are higher at the two ends than in the middle of the considered coastline. For example, the absolute value of the correlation coefficient between Δp and U_t can be above 0.3 for KPs between 500 and 800, and between 2500 and 3200, indicating that the correlation among these two parameters is non-negligible. Interestingly, a strong positive correlation is observed between Δp and U_t, in the south of the coastline, while they turn out to be negatively correlated in the north. The opposite phenomenon can be observed for the correlation between θ and U_t, which are negatively correlated in the south but positively correlated in the north. Second, the correlation between D_{min} and θ, and the correlation between Δp and θ are negative at almost all locations. This is partly due to the rapid decay of the typhoon intensity after the landfall. Because the southeast coast of China locates in the northwest of the WNP basin, large values of θ indicate the typhoons are entering the circular subregion from the land side, according to the definition of θ shown in Figure 1. Therefore, the larger θ is usually associated with the smaller intensity of typhoons, leading to the negative correlation between Δp and θ; similarly, since the occurrence of typhoons decreases with the distance from the typhoon to the coast, the typhoons coming from the land side tends to have a smaller value of D_{min} than those from the sea, that accounts for the negative correlation between D_{min} and θ. Third, the correlation coefficient between D_{min} and U_t, as well as that between Δp and U_t, on average, are at a level of 0.1.

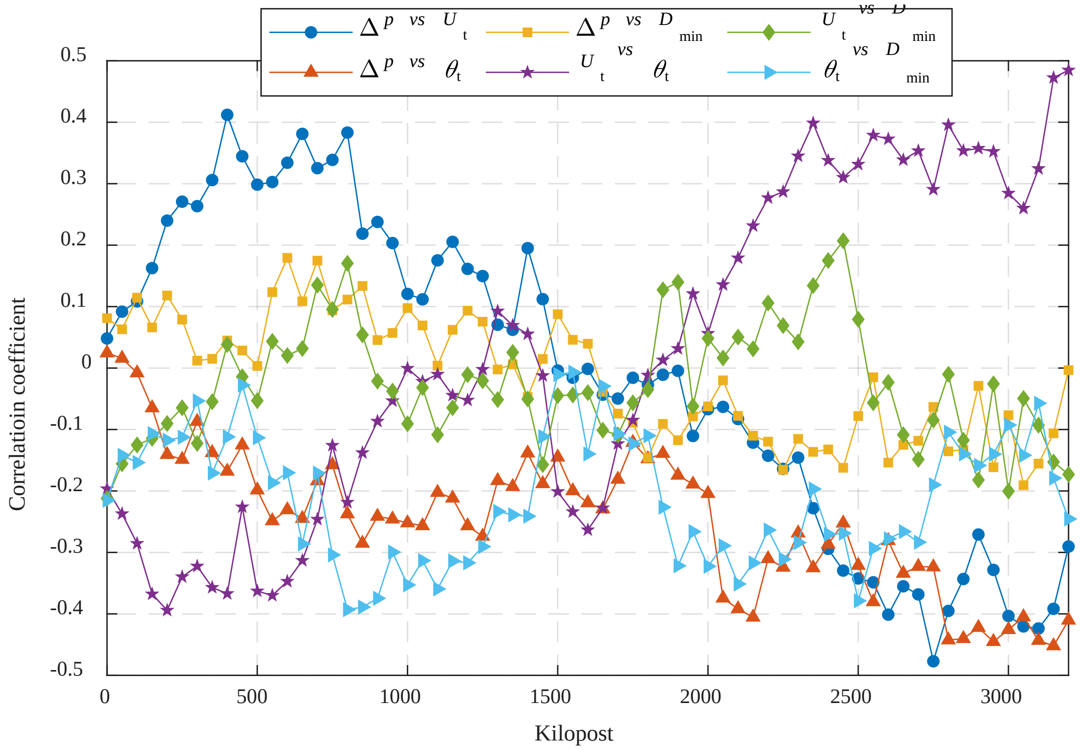

Figure 4 Variation of the correlation coefficients among typhoon key parameters with KP.

The identified dependence structure of the variables and the associated optimal copulas for the considered cities are listed in Table 4. Here, the "Clayton90/180/270" denotes the rotation version of the Clayton copula, and the "-asym" means the asymmetric copula constructed in the form of Eq.(3). It can be seen that the dominating order of variables and the identified copulas vary with different cities, indicating the complexity of the correlation among the typhoon key parameters. To examine whether the obtained copula model is able to represent the dependence structure of the parameters, the goodness-of-fit test is also performed. Here, the widely used Cramér-von Mises statistics (Genest et al., 2009) based on the Rosenblatt's probability integral transform is adopted for this test, and the P-value is listed in Table 4 as well. It can be seen that the P-values are greater than the significance level of 5%, which implies that the obtained copula model can be accepted to describe the dependence structure of these parameters (Genest et al., 2009).

Table 4 The identified dependence structure of typhoon key parameters.

City	Dominating order	Identified copulas	P-value
Shanghai	$\Delta p, D_{\min}, \theta, U_t$	C_{12}: Clayton270, $\lambda = 0.2865$ C_{13}: QS copula, $\lambda = 0.0503$ C_{14}: Clayton90, $\lambda = 0.9241$ $C_{23\|1}$: QS copula, $\lambda = -0.0395$ $C_{24\|1}$: Clayton90, $\lambda = 0.2951$ $C_{34\|12}$: QS copula, $\lambda = -0.1395$	0.06
Ningbo	$\Delta p, D_{\min}, \theta, U_t$	C_{12}: Clayton90, $\lambda = 0.3542$ C_{13}: QS copula, $\lambda = 0.1153$ C_{14}: Frank, $\lambda = -3.6652$ $C_{23\|1}$: QS copula, $\lambda = 0.0178$ $C_{24\|1}$: Frank, $\lambda = -0.5588$ $C_{34\|12}$: QS copula, $\lambda = 0.0454$	0.27
Wenzhou	$\theta, D_{\min}, U_t, \Delta p$	C_{12}: QS copula, $\lambda = 0.0183$ C_{13}: QS copula, $\lambda = 0.0443$ C_{14}: QS copula, $\lambda = 0.0470$ $C_{23\|1}$: Gumbel-asmy, $\lambda = 37.3523$, $\alpha = 0.1161$, $\beta = 0.2843$ $C_{24\|1}$: Clayton90-asmy, $\lambda = 26.4886$, $\alpha = 0.4697$, $\beta = 0.2246$ $C_{34\|12}$: Clayton-asmy, $\lambda = 33.5232$, $\alpha = 0.1457$, $\beta = 1$	0.52
Fuzhou	$\theta, D_{\min}, U_t, \Delta p$	C_{12}: QS copula, $\lambda = -0.0523$ C_{13}: QS copula, $\lambda = 0.0178$ C_{14}: QS copula, $\lambda = 0.0426$ $C_{23\|1}$: Clayton, $\lambda = 0.1338$ $C_{24\|1}$: Clayton, $\lambda = 0.1560$ $C_{34\|12}$: Clayton90-asmy, $\lambda = 57.1194$, $\alpha = 0.0814$, $\beta = 1$	0.07
Xiamen	$D_{\min}, \theta, U_t, \Delta p$	C_{12}: QS copula, $\lambda = -0.0550$ C_{13}: Clayton90, $\lambda = 0.1917$ C_{14}: Frank, $\lambda = -0.8383$ $C_{23\|1}$: QS copula, $\lambda = 0.0576$ $C_{24\|1}$: QS copula, $\lambda = 0.1370$ $C_{34\|12}$: Clayton90, $\lambda = 0.0974$	0.28
Shantou	$\Delta p, D_{\min}, \theta, U_t$	C_{12}: Clayton, $\lambda = 0.1102$ C_{13}: QS copula, $\lambda = 0.1434$ C_{14}: Frank, $\lambda = 0.9737$ $C_{23\|1}$: QS copula, $\lambda = 0.0385$ $C_{24\|1}$: Clayton90-asmy, $\lambda = 8.2832$, $\alpha = 0.1934$, $\beta = 1$ $C_{34\|12}$: QS copula, $\lambda = -0.0214$	0.85
Guangzhou	$\theta, \Delta p, U_t, D_{\min}$	C_{12}: QS copula, $\lambda = 0.0866$ C_{13}: QS copula, $\lambda = -0.0545$ C_{14}: QS copula, $\lambda = 0.0983$ $C_{23\|1}$: Gauss-asmy, $\lambda = 0.9197$, $\alpha = 0.1758$, $\beta = 0.7377$ $C_{24\|1}$: Clayton180, $\lambda = 0.2100$ $C_{34\|12}$: Frank, $\lambda = -0.1716$	0.10
Yangjiang	$U_t, \theta, \Delta p, D_{\min}$	C_{12}: QS copula, $\lambda = 0.0568$ C_{13}: Gumbel, $\lambda = 1.2731$	0.08

		C_{14}: Clayton, $\lambda = 0.1639$ $C_{23\|1}$: QS copula, $\lambda = 0.1189$ $C_{24\|1}$: QS copula, $\lambda = 0.0729$ $C_{34\|12}$: Student's t, $\lambda = 0.0253$, $\chi = 4.4300$	
Zhanjiang	U_t, θ, Δp, $D_{\min}$	C_{12}: QS copula, $\lambda = 0.1358$ C_{13}: Clayton-asmy, $\lambda = 13.8216$, $\alpha = 0.7706$, $\beta = 0.2409$ C_{14}: Clayton90, $\lambda = 0.1428$ $C_{23\|1}$: QS copula, $\lambda = 0.1220$ $C_{24\|1}$: QS copula, $\lambda = -0.0592$ $C_{34\|12}$: Clayton, $\lambda = 0.1661$	0.15

Thus, the joint probability distribution of the typhoon key parameters can be readily obtained according to Eq.(1). For illustration, the observed scatterplots and modeled two-dimensional marginal probability distributions for pairs of the typhoon key parameters at Wenzhou are shown in Figure 5. The visual inspection demonstrates that the correlation patterns among these parameters can be well captured by the copula method. Similar observations are yielded for other cities but are not displayed here due to space limitations. To quantify the effectiveness of using the Copula method in modeling the joint probability distribution, the statistical moments up to the fourth order of both the observation and the joint probability distribution are compared. Specifically, the observed and modeled second, third and fourth standardized mixed moments among the parameters are estimated,

$$m_{ij} = \overline{\frac{\left(x_i - \overline{x_i}\right)}{\sigma_i}\frac{\left(x_j - \overline{x_j}\right)}{\sigma_j}}, \tag{5}$$

$$m_{ijk} = \overline{\frac{\left(x_i - \overline{x_i}\right)}{\sigma_i}\frac{\left(x_j - \overline{x_j}\right)}{\sigma_j}\frac{\left(x_k - \overline{x_k}\right)}{\sigma_k}}, \tag{6}$$

$$m_{ijkl} = \overline{\frac{\left(x_i - \overline{x_i}\right)}{\sigma_i}\frac{\left(x_j - \overline{x_j}\right)}{\sigma_j}\frac{\left(x_k - \overline{x_k}\right)}{\sigma_k}\frac{\left(x_l - \overline{x_l}\right)}{\sigma_l}}, \tag{7}$$

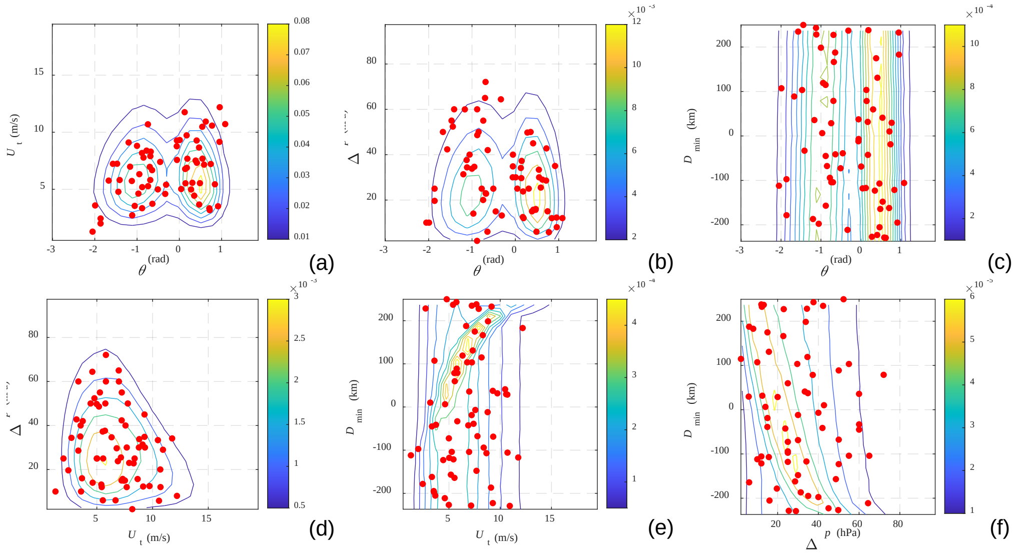

Figure 5 Observed scatterplots (red points) and modeled contours of 2D marginal probability distribution.

where σ_i, σ_j, σ_k and σ_l are the standard deviation of each component of $\boldsymbol{X}$, $\boldsymbol{X}=\left(\Delta p, D_{\min}, U_t, \theta\right)^{\mathrm{T}}$, and $\overline{(\cdot)}$ is the statistical average operator. The observed and simulated moments for all the considered cities are collected and compared in Figure 6. It can be seen from Figure 6(a) that the points paired by the observed and modeled 2nd-order moments align well with the diagonal. The points for the 3$^{\text{rd}}$ and 4th-order moments are more scattered, partly owing to the limited size of samples. Despite this, the modeled moments are, in general, consistent with the observed ones. The linear regression between the observed and modeled statistical moments finds that the slope and intercept are 0.987 and 0.023 for the second moment, 0.861 and -0.059 for the third moment and 0.828 and -0.084 for the fourth moment. The slopes are close to the unit and the intercepts are close to zero. These demonstrate the adequacy of the Copula method.

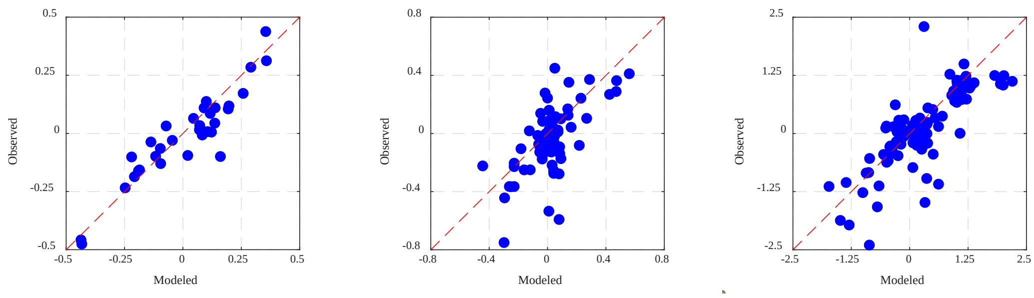

(a) 2nd moments (b) 3rd moments (c) 4th moments

Figure 6 Observed and modeled moments among the typhoon key parameters.

Typhoon hazard assessment

As aforementioned, the typhoon local track can be determined by $D_{\min}$, U_t and θ. Besides, a wind field model is utilized to calculate the typhoon-induced surface wind at the interested site. Various typhoon wind field models have been studied, ranging from tractable parametric models (Holland, 1980; Willoughby and Rahn, 2004) to full-physics models (Kepert and Wang, 2001; Zhang et al., 2022). As the main objective of this study is to investigate the influence of the correlation of the typhoon key parameters on the wind hazard, for simplicity, the parametric model used by Georgiou (1985) and Cui and Caracoglia (2016) is considered for the gradient wind field in this study. Georgiou's model is based on the Holland pressure profile and accounts for the influence of the typhoon translation velocity,

$$V_g = \frac{1}{2}\left(U_t \sin\alpha - fr\right) + \sqrt{\frac{1}{4}\left(U_t \sin\alpha - fr\right)^2 + \frac{100B\Delta p}{\rho}\left(\frac{R_{\max}}{r}\right)^B \exp\left[-\left(\frac{R_{\max}}{r}\right)^B\right]}, \tag{8}$$

where α denotes the angle rotating from the typhoon heading to the position of the interested site in the clockwise direction, f is the Coriolis frequency $\left(=2\Omega\sin\phi\right)$, $\Omega = 7.29\times10^{-5}\,\mathrm{rad/s}$, ϕ is the latitude of the interested site, r is the distance from the typhoon center to the interested site. Note that besides the probability distribution model for Δp, $D_{\min}$, U_t and θ, given the previous section, the information of $R_{\max}$ and B needs to be supplemented. They are related to Δp and ϕ using the statistical relation developed by Fang et al. (2018b), i.e.,

$$\ln R_{\max} = 5.51\Delta p^{-0.117} + 6.707\times10^{-3}\phi + \sigma_{\ln R_{\max}}\varepsilon_{\ln R_{\max}}, \tag{9}$$

$$\sigma_{\ln R_{\max}} = -1.836\times10^{-4}\Delta p + 0.364, \tag{10}$$

and

$$B = 4.1025\times10^{-5}\Delta p^2 + 0.0293\Delta p + 0.7959\ln R_{\max} - 4.601 + \sigma_B\varepsilon_B, \tag{11}$$

$$\sigma_B = -0.0027\Delta p - 0.1311\ln R_{\max} + 0.8815, \tag{12}$$

where $\sigma_{\ln R_{\max}}$ and σ_B are the standard deviation of $\ln R_{\max}$ and B, $\varepsilon_{\ln R_{\max}}$ and ε_B are the standard normal random variables. To convert the gradient wind to the surface and to consider the sea-land transition, the speed reduction factor proposed by Chen and Duan (2018) is applied here. It is assumed the simulated wind speed is comparable to the wind speed averaged over a period of 10 min. When a typhoon propagates along the track, by simulating the surface wind speeds at the interested site at each time step, the typhoon-induced wind speed history and its maximum value during that specific typhoon impacting the site can be obtained. To validate the adequacy of the wind field model, the history of the surface wind speed of Typhoon Hagupit in 2008 at Yangjiang (21.83° N, 111.97° E) is simulated and compared to the surface observation (Hong et al., 2016). In the simulation, the information on track and central pressure deficit is extracted from the CMA best track dataset; B and $R_{\max}$ are calculated using the deterministic relations in Eqs. (9) and (11). As is presented in Figure 7, the simulated history of surface wind agrees well with the observation.

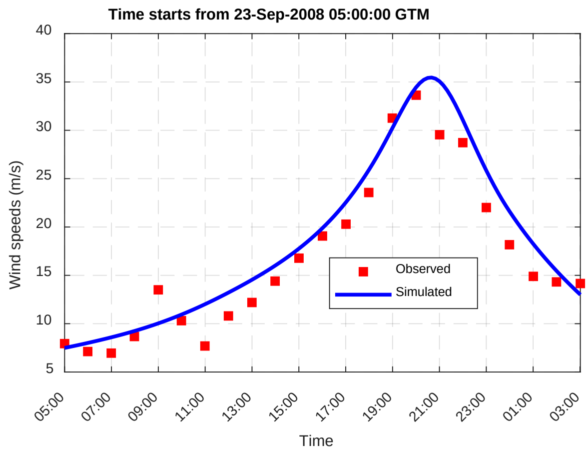

Figure 7 The observed and simulated surface wind speed of Typhoon Hagupit (2008) at Yangjiang.

To summarize, the basic random variables involved in the typhoon model include Δp, $D_{\min}$, U_t, θ, $\varepsilon_{\ln R_{\max}}$ and ε_B, and the typhoon model works as the mapping from the probability space of the basic random variables to that of the maximum surface wind speed during the impact of a single typhoon, denoted by V_m. For clarity, let $F_m(v)$ and $p_m(v)$ denote the cumulative distribution function (CDF) and PDF of V_m. To estimate $F_m(v)$ and $p_m(v)$, the Monte Carlo simulation is adopted in this study.

Since the occurrence of typhoons is a typical point process, it is desired to represent the potential typhoon wind hazard by values associated with certain return periods. For this purpose, the occurrence of typhoons is assumed to be a Poisson process with an annual occurrence rate ξ. Values of ξ at each considered city can be found in Table 2. Therefore, the number of typhoons occurring during the time interval of one year, denoted by N, obeys the Poisson distribution with the parameter of ξ, i.e.,

$$\Pr\{N=k\}=\frac{\xi^k \mathrm{e}^{-\xi}}{k!},\quad k=0,1,2,\cdots, \tag{13}$$

where $\Pr\{\cdot\}$ probability of an event. The CDF of the annual maximum typhoon-induced surface wind, denoted by $F_{m1}(v)$, can be derived as follows,

$$F_{m1}(v)=\sum_{k=0}^{\infty}\Pr\{N=k\}F_m(v)^k=\sum_{k=0}^{\infty}\frac{\left[\xi F_m(v)\right]^k \mathrm{e}^{-\xi}}{k!}=\mathrm{e}^{-\xi}\cdot \mathrm{e}^{\xi F_m(v)}=\mathrm{e}^{-\xi\left[1-F_m(v)\right]}. \tag{14}$$

Consequently, the wind speed associated with the return period of T years can be estimated as

$$v_T=F_{m1}^{-1}\left(1-\frac{1}{T}\right)=F_m^{-1}\left[1+\frac{1}{\xi}\ln\left(1-\frac{1}{T}\right)\right]\approx F_m^{-1}\left(1-\frac{1}{\xi T}\right), \tag{15}$$

where the use of the approximation of $\ln(1-1/T)\approx -1/T$ is made for large values of T.

Results

Influence of the correlation on the typhoon wind hazard

Two models are considered to investigate the influence of the correlation among the typhoon key parameters on the typhoon wind hazard. In the first model (TWHM1), the correlations among Δp, $D_{\min}$, U_t, θ are considered using the Copula method illustrated above, and one million samples for the basic random variables (i.e., Δp, $D_{\min}$, U_t, θ, $\varepsilon_{\ln R_{\max}}$ and ε_B) are generated at each location on the coastline. Subsequently, the Monte Carlo simulation is utilized to derive values of v_T for different values of T. The second model (TWHM2) differs from the TWHM1 by ignoring the correlations among the typhoon key parameters and treating them as independent random variables.

The comparison between the histograms of the annual maximum typhoon-induced surface wind by TWHM1 and those by TWHM2 at the considered cities are shown in Figure 8. It can be observed that the overall shape of the histograms by TWHM1 agrees with that of TWHM2, but the TWHM1 produces higher peak values of PDF in Shanghai, Ningbo and Wenzhou but leads to smaller peak values of PDF at other locations compared to TWHM2. To better appreciate the difference between the wind hazards estimated by TWHM1 and TWHM2, the variation of the wind speeds with the return period is displayed in Figure 9. The probability distributions of annual maximum wind speed estimated by TWHM2 have a thicker upper tail and lead to higher wind hazards at Shanghai, Ningbo and Wenzhou. Especially at Shanghai, the difference between the wind speeds for the 50-year return period is 2.5 m/s, indicating a relative difference of around 8.33%. However, at Xiamen, Shantou, Guangzhou and Zhanjiang, the wind hazards estimated by TWHM1 are greater than TWHM2. At Fuzhou and Yangjiang, the difference between the curves of the two models is not significant.

The variations of v_{50} and v_{100} for both models with KP are displayed in Figure 10 (a) and (b), and their relative differences are presented in Figure 10 (c) and (d). In the south of the coastline, v_{50} estimated by TWHM1 is larger than TWHM2, indicating that ignoring the correlations among typhoon key parameters can underestimate the wind hazards. In the north of the coastline, however, ignoring the correlations might lead to greater wind hazards compared to the fully correlated case. Despite the relative difference between TWHM1 and TWHM2 in the middle of the coastline is limited, it could be larger than 5% in both the north and south end of the considered coastline. For example, the relative difference is -6.93% at KP = 200 and 7.7% at KP = 3050. Similar observations can be made from the comparison on v_{100}. Recently, Wu et al. (2021) investigated the influence of the correlation between typhoon key parameters on v_T using the Nataf transformation. They found the change in v_{50} and v_{100} caused by considering the correlations is less than 2% at nine cities on the southeast coast of China. The difference between Wu et al. (2021) and the present study might be owing to two reasons. First, the Nataf transformation is identical to the Copula method if the Gaussian Copula function is used to model the dependence structure of random variables (Montes-Iturrizaga and Heredia-Zavoni, 2016), but as indicated by Table 1 and Table 4, various Copula functions including the Gaussian Copula function are considered in the present study to better capture other possible dependence structures. Therefore, the change of v_T caused by considering the correlations by the Nataf transformation could differ from that by the Copula method. Second, in determining the circular region, the authors assume the radius of the circular region equals 250 km, while Wu et al. (2021) used a value of 500 km. This indicates the dataset used in Wu et al. (2021) is not identical to that of the present study regarding the probability characteristics. This could in part contribute to the fact that the present study draws a different conclusion regarding the influence of the correlations on the typhoon wind hazard.

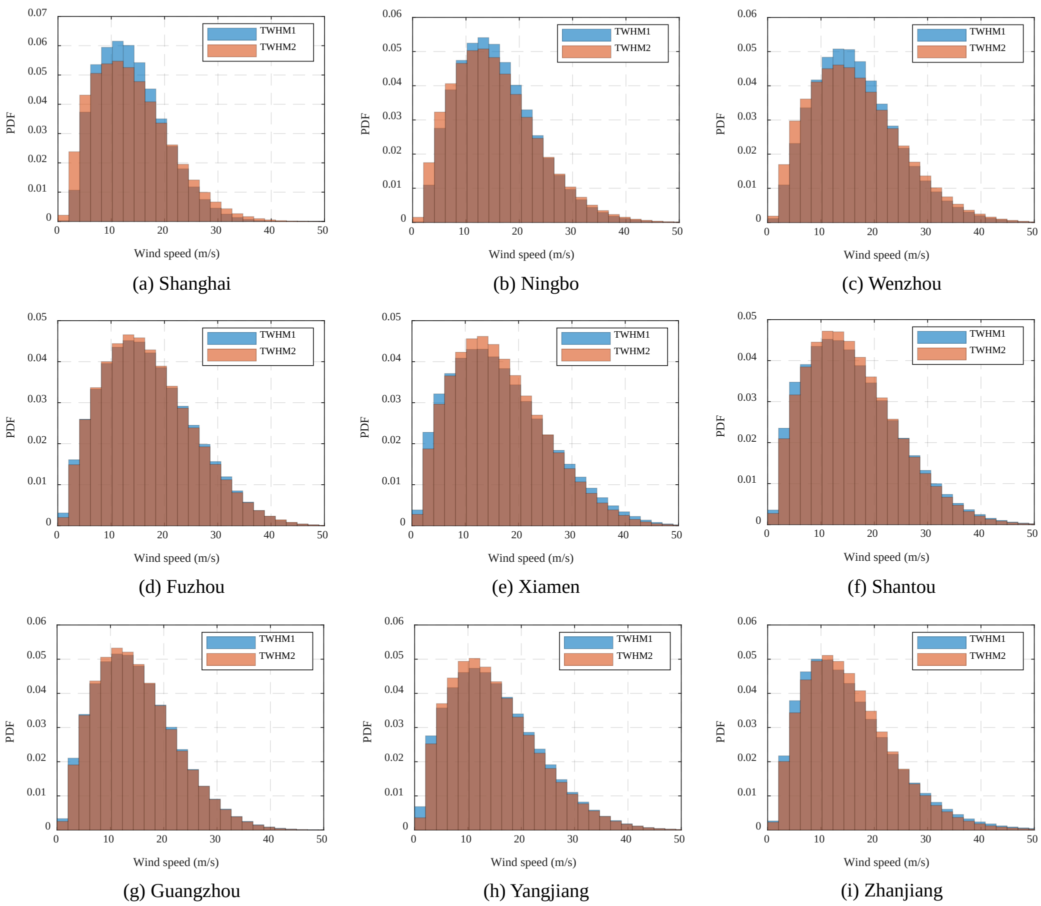

Figure 8 PDFs of the annual maximum typhoon-induced surface wind at considered cities.

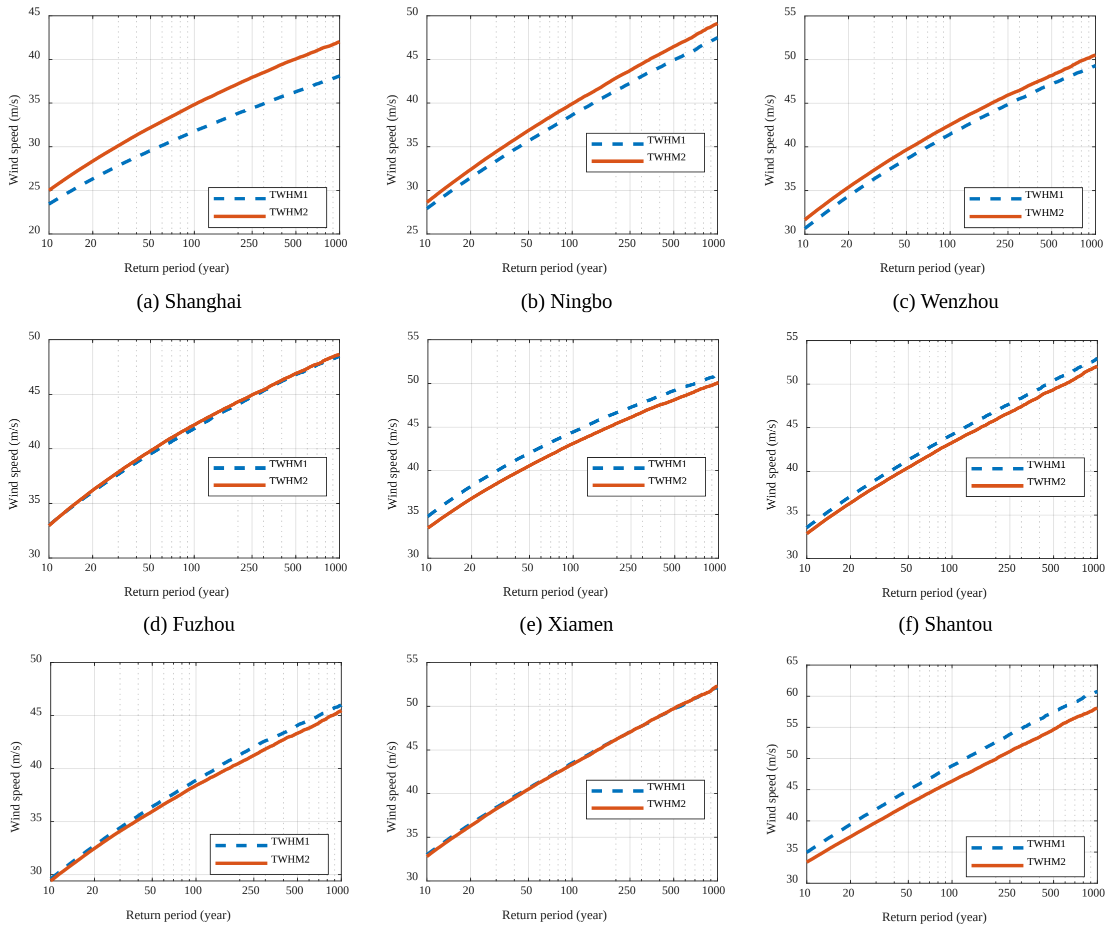

(a) Shanghai (b) Ningbo (c) Wenzhou

(d) Fuzhou (e) Xiamen (f) Shantou

(g) Guangzhou (h) Yangjiang (i) Zhanjiang

Figure 9 CDFs of the annual maximum typhoon-induced surface wind at considered cities.

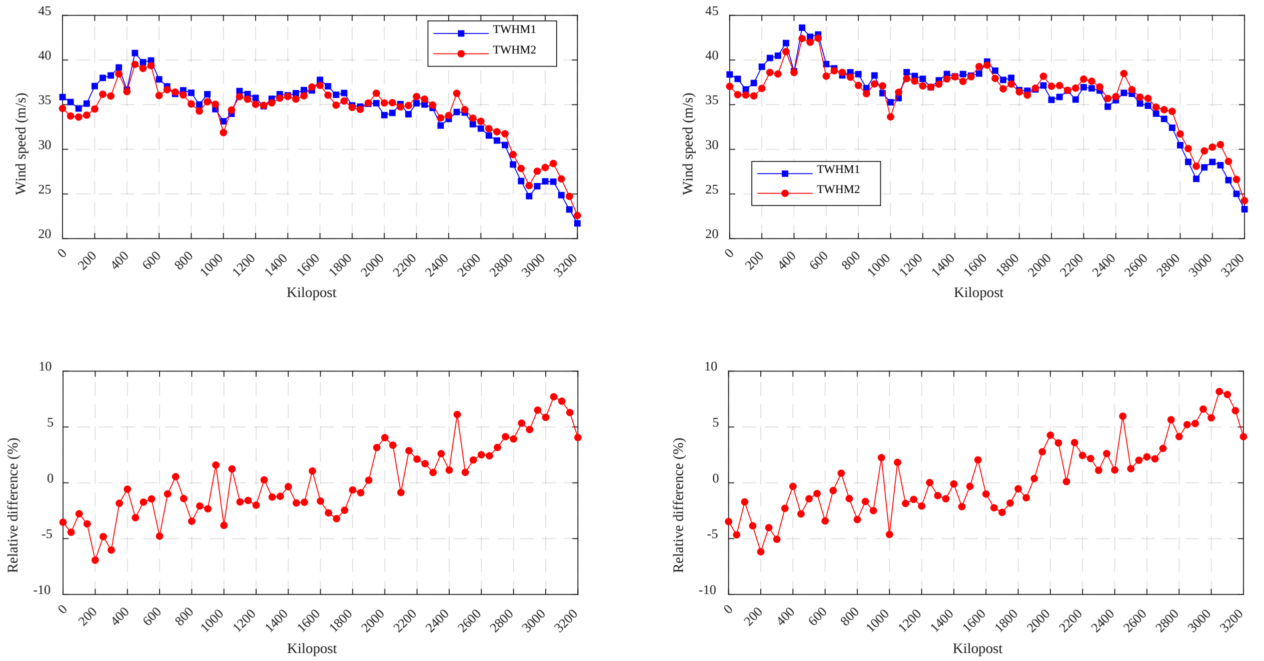

(d) Relative difference for the wind speed associated with T = 100 years

Figure 10 Comparison between vT by TWHM1 and TWHM2 for T = 50 years and T = 100 years.

Sensitivity analysis

The previous subsection shows that in the south ignoring the correlation will underestimate v_T but in the north it leads to the overestimation. To further investigate the cause of this opposite effect, the sensitivity of v_{50} to the correlations between every two key parameters is analyzed. From the four typhoon key parameters, six pairs of two distinct key parameters can be formed, i.e., $(\Delta p, D_{\min})$, $(\Delta p, U_t)$, $(\Delta p, \theta)$, $(D_{\min}, U_t)$, $(D_{\min}, \theta)$ and (U_t, θ). First, the Copula method is used again to generate the joint probability distributions for each pair of parameters. Since only the correlation between two variables is considered in this case, the joint PDF can be expressed as

$$f(x_1, x_2) = f_1 f_2 c_{12}(F_1, F_2) \tag{16}$$

Since the marginal distributions of all variables for different sites have been modeled previously, only the dependence structure needs to be established. The identified optimal bivariate copulas for the six pairs of variables for different cities are given in Table 5. Then, six typhoon wind hazard models, denoted as TWHMSA1-6, are considered to investigate the influence of the correlation of each pair on v_{50}. The probability distribution model assigned for each model is tabulated in Table 6. In analogy to TWHM1 and 2, values of v_{50} associated with TWHMSAs are estimated using the Monte Carlo simulation with one million samples.

Table 5 The identified optimal bivariate copulas for pairs of parameters.

City	Pairs of variable	Identified copulas	
Shanghai	$\theta \sim U_t$	QS copula,	$\lambda = 0.0978$
	$\theta \sim \Delta p$	QS copula,	$\lambda = 0.0503$
	$\theta \sim D_{\min}$	QS copula,	$\lambda = -0.0449$
	$U_t \sim \Delta p$	Clayton90,	$\lambda = 0.9241$
	$U_t \sim D_{\min}$	Gumbel-asym,	$\lambda = 24.1311$, $\alpha = 1$, $\beta = 0.0589$
	$\Delta p \sim D_{\min}$	Clayton270,	$\lambda = 0.2865$
Ningbo	$\theta \sim U_t$	QS copula,	$\lambda = -0.0093$
	$\theta \sim \Delta p$	QS copula,	$\lambda = 0.1153$
	$\theta \sim D_{\min}$	QS copula,	$\lambda = -0.0280$
	$U_t \sim \Delta p$	Frank,	$\lambda = -3.6652$
	$U_t \sim D_{\min}$	Gumbel-asym,	$\lambda = 3.1091$, $\alpha = 1$, $\beta = 0.1177$
	$\Delta p \sim D_{\min}$	Clayton90,	$\lambda = 0.3542$

Wenzhou	$\theta \sim U_t$	QS copula, $\lambda = 0.0443$
	$\theta \sim \Delta p$	QS copula, $\lambda = 0.0470$
	$\theta \sim D_{\min}$	QS copula, $\lambda = 0.0183$
	$U_t \sim \Delta p$	Clayton90-asym, $\lambda = 15.8194$, $\alpha = 0.2004$, $\beta = 1$
	$U_t \sim D_{\min}$	Gumbel-asym, $\lambda = 40.0262$, $\alpha = 0.3277$, $\beta = 0.1369$
	$\Delta p \sim D_{\min}$	Clayton90, $\lambda = 0.1939$
Fuzhou	$\theta \sim U_t$	QS copula, $\lambda = 0.0178$
	$\theta \sim \Delta p$	QS copula, $\lambda = 0.0426$
	$\theta \sim D_{\min}$	QS copula, $\lambda = -0.0523$
	$U_t \sim \Delta p$	Clayton180-asym, $\lambda = 55.3364$, $\alpha = 0.1178$, $\beta = 0.5837$
	$U_t \sim D_{\min}$	Gumbel-asym, $\lambda = 29.5960$, $\alpha = 1$, $\beta = 0.0299$
	$\Delta p \sim D_{\min}$	Gumbel-asym, $\lambda = 6.6937$, $\alpha = 0.1157$, $\beta = 0.2536$
Xiamen	$\theta \sim U_t$	QS copula, $\lambda = 0.0587$
	$\theta \sim \Delta p$	QS copula, $\lambda = 0.1413$
	$\theta \sim D_{\min}$	QS copula, $\lambda = -0.0550$
	$U_t \sim \Delta p$	Clayton, $\lambda = 0.1066$
	$U_t \sim D_{\min}$	Clayton90, $\lambda = 0.1917$
	$\Delta p \sim D_{\min}$	Frank, $\lambda = -0.8383$
Shantou	$\theta \sim U_t$	QS copula, $\lambda = 0.0047$
	$\theta \sim \Delta p$	QS copula, $\lambda = 0.1434$
	$\theta \sim D_{\min}$	QS copula, $\lambda = 0.0428$
	$U_t \sim \Delta p$	Frank, $\lambda = 0.9737$
	$U_t \sim D_{\min}$	Clayton90-asym, $\lambda = 48.8509$, $\alpha = 0.1156$, $\beta = 1$
	$\Delta p \sim D_{\min}$	Clayton, $\lambda = 0.1102$
Guangzhou	$\theta \sim U_t$	QS copula, $\lambda = -0.0545$
	$\theta \sim \Delta p$	QS copula, $\lambda = 0.0866$
	$\theta \sim D_{\min}$	QS copula, $\lambda = 0.0983$
	$U_t \sim \Delta p$	Gauss-asym, $\lambda = 0.9013$, $\alpha = 0.7468$, $\beta = 0.2206$
	$U_t \sim D_{\min}$	Clayton180, $\lambda = 0.0354$
	$\Delta p \sim D_{\min}$	Clayton180, $\lambda = 0.2435$
Yangjiang	$\theta \sim U_t$	QS copula, $\lambda = 0.0568$
	$\theta \sim \Delta p$	QS copula, $\lambda = 0.1245$
	$\theta \sim D_{\min}$	QS copula, $\lambda = 0.0924$
	$U_t \sim \Delta p$	Gumbel, $\lambda = 1.2731$
	$U_t \sim D_{\min}$	Clayton, $\lambda = 0.1639$
	$\Delta p \sim D_{\min}$	Gumbel-asym, $\lambda = 4.0645$, $\alpha = 0.0583$, $\beta = 0.7661$
Zhanjiang	$\theta \sim U_t$	QS copula, $\lambda = 0.1358$
	$\theta \sim \Delta p$	QS copula, $\lambda = 0.1452$
	$\theta \sim D_{\min}$	QS copula, $\lambda = 0.0413$
	$U_t \sim \Delta p$	Clayton-asym, $\lambda = 13.8216$, $\alpha = 0.7706$, $\beta = 0.2409$
	$U_t \sim D_{\min}$	Clayton90, $\lambda = 0.1428$
	$\Delta p \sim D_{\min}$	Clayton90, $\lambda = 0.1446$

Table 6 Probability distribution models assigned for TWHMSAs.

Model	Probability model of the typhoon key parameters
TWHMSA1	The correlation between (U_t, θ) is considered by the Copula method; other parameters are assumed as independent variables.
TWHMSA2	The correlation between $(\Delta p, \theta)$ is considered by the Copula method; other parameters are assumed as independent variables.
TWHMSA3	The correlation between $(D_{\min}, \theta)$ is considered by the Copula method; other parameters are assumed as independent variables.
TWHMSA4	The correlation between $(\Delta p, U_t)$ is considered by the Copula method; other parameters are assumed as independent variables.
TWHMSA5	The correlation between $(D_{\min}, U_t)$ is considered by the Copula method; other parameters are assumed as independent variables.
TWHMSA6	The correlation between $(\Delta p, D_{\min})$ is considered by the Copula method; other parameters are assumed as independent variables.

The relative difference between the v_{50} estimated by TWHMSAs and that by TWHM2 is presented in Figure 11. Because in TWHM2 the typhoon key parameters are treated as independent random variables, the deviation of v_{50} by TWHMSAs from that by TWHM2 indicates the importance of the correlation of the associated parameter pairs. The quite flat feature of the variation curve of the relative difference with the KP for (U_t, θ), $(\Delta p, \theta)$, $(D_{\min}, \theta)$ and $(D_{\min}, U_t)$ demonstrates that the correlation between these parameter pairs plays a minor role in influencing the typhoon wind hazards. Also, as indicated by Figure 11(f), the relative difference for $(\Delta p, D_{\min})$ is in general negative, suggesting that not including their correlation tends to overestimate the wind hazards. Moreover, similar to THWM1 where the full correlation among the typhoon key parameters is considered, including the correlation between $(\Delta p, U_t)$ can lead to the underestimation in the south of the coast but cause the overestimation in the north of the coast. The above analyses indicate the opposite effect of considering the correlation on v_{50} is mainly associated with the correlation between $(\Delta p, U_t)$. Because the wind surface wind field is comprised of the axisymmetric component controlled by Δp and the non-axisymmetric component associated with the typhoon motion controlled by U_t, increasing both Δp and U_t can lead to the increase of the extreme surface wind speed. As indicated by Figure 4, Δp and U_t are positively correlated in the south and negatively correlated in the north. Therefore, if the correlation between Δp and U_t is restored, greater extreme wind speed wind will be produced in the south and smaller extreme wind speed will be observed in the north.

Further, the variation of the maximum relative difference between the v_T estimated by THWM2 and THWMSAs on the coastline with the return period is displayed in Figure 12. Except for $(\Delta p, U_t)$ and $(\Delta p, D_{\min})$, all the maximum relative differences are no larger than 3%. To conclude, the above analyses suggest that in modeling the joint probability distribution of typhoon key parameters, the correlations among Δp, $D_{\min}$ and U_t on the typhoon wind hazard might not be ignored because their correlation can result in a change of more than 5% in the typhoon wind hazards at some locations; on the other hand, the influence of the correlation between θ with other parameters on the typhoon wind hazards is limited.

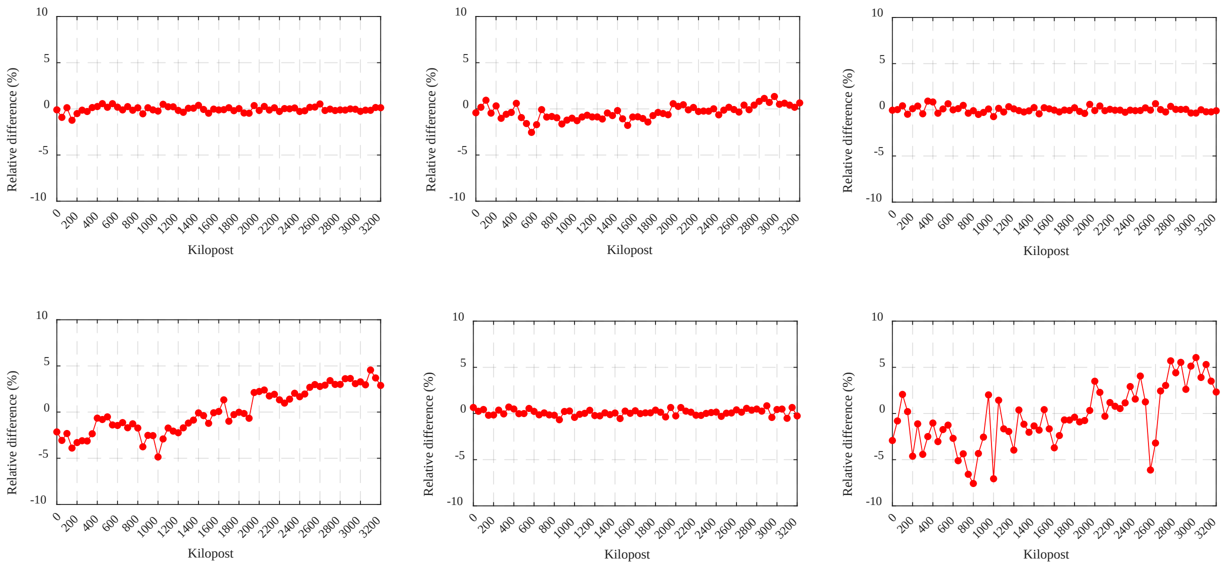

(f) Δp vs $D_{\min}$

Figure 11 Relative difference between v50 by THWM2 and v50 by THWMSAs.

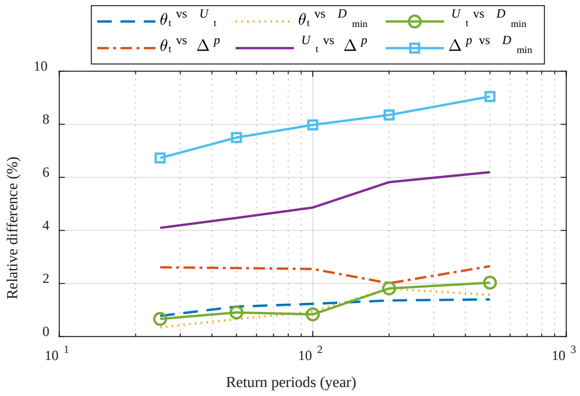

Figure 12 The maximum relative difference between the vT estimated by THWM1 and THWMSAs.

Conclusions

This paper develops the Copula-method-based probability distribution model for the typhoon key parameters, which can be potentially used to assess the typhoon hazard on the southeast coast of China. The conclusions which could be drawn from this study go as follows:

1) Analyses of the measurements of the typhoon key parameters show that the correlation coefficients are higher than 0.3 at considerable locations. Also, the correlations are higher at the two ends than in the middle of the considered coastline. The probabilistic dependence characteristics of the typhoon key parameters vary with sites, and the C-vine copula can be adopted to describe the dependence structure of these parameters. The comparison between observed and modeled moments demonstrates the adequacy of the Copula model.
2) Monte Carlo simulation is carried out to estimate the wind speeds associated with 50-year and 100-year return periods for both including and excluding the correlation among the typhoon key parameters on the southeast coastline of China. The comparison shows that the difference between the two cases is limited (generally within 5%) in the middle of the coastline. However, the relative difference of v_{50} and v_{100} between considering and ignoring the correlations between parameters could be up to 7% at two ends of the considered coastline.
3) The sensitivity analysis demonstrates that the influence of correlations among Δp , D_{min} and U_{t} on the typhoon wind hazard should be included as their correlation can result in a change of more

than 5% in the typhoon wind hazards at some places; on the other hand, the influence of the correlation between θ with other parameters on the typhoon wind hazards is limited.

Despite the Copula method is proven to be effective in capturing the correlated structure of the typhoon key parameters and being potentially useful in assessing the typhoon hazard, some important issues have not been considered by the present study yet. For instance, as aforementioned, the probabilistic characteristics, as well as the correlation, of the key parameters could vary with time because of the climate change. This could be accounted for by dividing the historical data into separate climatological parts and applying the proposed method to each part. Moreover, the wind field model adopted in this study is a simple parametric model. Though the comparison to the observation proves the validity of the model in part, it is desired to improve the proposed typhoon hazard assessment method by replacing the parametric model with the high-fidelity model. These issues will be considered in future work.

Data Availability Statement

All data, models, or code that support the findings of this study are available from the corresponding author upon reasonable request.

Acknowledgments

The financial support from the Fundamental Research Funds for the Central Universities of China (Nos. JZ2022HGQA0168, PA2022GDSK0063), the Natural Science Foundation of Jiangsu Province (Grant No. BK20220357), and the Natural Science Foundation of the Jiangsu Higher Education Institutions (Grant No. 22KJB560005) are highly appreciated.

References

Aas, K., Czado, C., Frigessi, A., Bakken, H., 2009. Pair-copula constructions of multiple dependence. Insurance: Mathematics and Economics 44 (2), 182-198.

Batts, M.E., Russell, L.R., Simiu, E., 1980. Hurricane Wind Speeds in the United-States. J. Struct. Div.-Asce 106, 2001–2016.

Candela, A. and Aronica, G.T., 2017. Probabilistic flood hazard mapping using bivariate analysis based on copulas. ASCE-ASME Journal of Risk and Uncertainty in Engineering Systems, Part A: Civil Engineering, 3(1), p.A4016002. https://doi.org/10.1061/AJRUA6.0000883

Chen, Y., Duan, Z., 2018. A statistical dynamics track model of tropical cyclones for assessing typhoon wind hazard in the coast of southeast China. J. Wind Eng. Ind. Aerodyn. 172, 325–340. https://doi.org/10/gcwzqp

Cui, W., Caracoglia, L., 2016. Exploring hurricane wind speed along US Atlantic coast in warming climate and effects on predictions of structural damage and intervention costs. Eng. Struct. 122, 209–225. https://doi.org/10.1016/j.engstruct.2016.05.003

Dißmann, J., Brechmann, E.C., Czado, C., Kurowicka, D., 2013. Selecting and estimating regular vine copulae and application to financial returns. Computational Statistics & Data Analysis 59, 52-69.

Emanuel, K., Ravela, S., Vivant, E., Risi, C., 2006. A statistical deterministic approach to hurricane risk assessment. Bull. Am. Meteorol. Soc. 87, 299-+. https://doi.org/10.1175/Bams-87-3-299

Fang, G., Zhao, L., Cao, S., Ge, Y., Pang, W., 2018a. A novel analytical model for wind field simulation under typhoon boundary layer considering multi-field correlation and height-dependency. J. Wind Eng. Ind. Aerodyn. 175, 77–89. https://doi.org/10/gdh25v

Fang, G., Zhao, L., Song, L., Liang, X., Zhu, L., Cao, S., Ge, Y., 2018b. Reconstruction of radial parametric pressure field near ground surface of landing typhoons in Northwest Pacific Ocean. J. Wind Eng. Ind. Aerodyn. 183, 223–234. https://doi.org/10.1016/j.jweia.2018.10.020

Fazeres-Ferradosa, T., Taveira-Pinto, F., Vanem, E., Reis, M.T., Neves, L.d., 2018. Asymmetric copula-based distribution models for met-ocean data in offshore wind engineering applications. Wind Engineering 42 (4), 304-334.

Fang, G., Zhao, L., Cao, S., Zhu, L., Ge, Y., 2020. Estimation of tropical cyclone wind hazards in coastal regions of China. Nat. Hazards Earth Syst. Sci. 20, 1617–1637. https://doi.org/10/gnbfk7

Genest, C., Remillard, B., Beaudoin, D., 2009. Goodness-of-fit tests for copulas: a review and a power study. Insurance Mathematics & Economics. 44 (2),199-213.

Georgiou, P.N., 1985. Design Wind Speeds In Tropical Cyclone-prone Regions. The University of Western Ontario, London, Ontario.

Georgiou, P.N., Davenport, A.G., Vickery, B.J., 1983. Design Wind Speeds in Regions Dominated by Tropical Cyclones. J. Wind Eng. Ind. Aerodyn. 13, 139–152. https://doi.org/10.1016/0167-6105(83)90136-8

García-Portugués, E., Crujeiras, R.M., González-Manteiga, W., 2013. Exploring wind direction and SO2 concentration by circular–linear density estimation. Stochastic Environmental Research and Risk Assessment 27 (5), 1055-1067.

Holland, G.J., 1980. An Analytic Model of the Wind and Pressure Profiles in Hurricanes. Mon. Weather Rev. 108, 1212–1218. https://doi.org/10.1175/1520-0493(1980)108<1212:Aamotw>2.0.Co;2

Hong, H.P., Li, S.H., Duan, Z.D., 2016. Typhoon Wind Hazard Estimation and Mapping for Coastal Region in Mainland China. Nat. Hazards Rev. 17. https://doi.org/10.1061/(Asce)Nh.1527-6996.0000210

Hong, X., Hong, H.P., Li, J., 2019. Solution and validation of a three dimensional tropical cyclone boundary layer wind field model. J. Wind Eng. Ind. Aerodyn. 193, 103973. https://doi.org/10/gm88jw

Hong, X., Li, J., 2022. Typhoon hazard assessment at site-specific scale based on the probability density evolution method and its application at Southeast Coast of China. Sci. CHINA Technol. Sci. https://doi.org/10.1007/s11431-021-2067-x

Hong, X., Li, J., 2021. A beta-advection typhoon track model and its application for typhoon hazard assessment. J. Wind Eng. Ind. Aerodyn. 208, 104439. https://doi.org/10/ghr6tn

Hu, X., Fang, G., Yang, J., Zhao, L. and Ge, Y., 2023. Simplified models for uncertainty quantification of extreme events using Monte Carlo technique. Reliability Engineering & System Safety, 230, p.108935. https://doi.org/10.1016/j.ress.2022.108935

Ishihara, T., Siang, K.K., Leong, C.C., Fujino, Y., 2005. Wind Field Model and Mixed Probability Distribution Function for Typhoon Simulation. Presented at the The Sixth Asia-Pacific Conference on Wind Engineering, Seoul, pp. 412–426.

Jäger, W.S. and Nápoles, O.M., 2017. A vine-copula model for time series of significant wave heights and mean zero-crossing periods in the North Sea. ASCE-ASME Journal of Risk and Uncertainty in Engineering Systems, Part A: Civil Engineering, 3(4), p.04017014. https://doi.org/10.1061/AJRUA6.0000917

Kepert, J., Wang, Y.Q., 2001. The dynamics of boundary layer jets within the tropical cyclone core. Part II: Nonlinear enhancement. J. Atmospheric Sci. 58, 2485–2501. https://doi.org/10.1175/1520-0469(2001)058<2485:Tdoblj>2.0.Co;2

Khajwal, A.B. and Noshadravan, A., 2020. Probabilistic hurricane wind-induced loss model for risk assessment on a regional scale. ASCE-ASME Journal of Risk and Uncertainty in Engineering Systems, Part A: Civil Engineering, 6(2), p.04020020. https://doi.org/10.1061/AJRUA6.0001062

Li, S.H., Hong, H.P., 2015a. Observations on a Hurricane Wind Hazard Model Used to Map Extreme Hurricane Wind Speed. J. Struct. Eng. 141. https://doi.org/10.1061/(Asce)St.1943-541x.0001217

Li, S.H., Hong, H.P., 2015b. Use of historical best track data to estimate typhoon wind hazard at selected sites in China. Nat. Hazards 76, 1395–1414. https://doi.org/10.1007/s11069-014-1555-z

Lombardo, F.T. and Ayyub, B., 2017. Approach to estimating near-surface extreme wind speeds with climate change considerations. ASCE-ASME Journal of Risk and Uncertainty in Engineering Systems, Part A: Civil Engineering, 3(3), p.A4017001. https://doi.org/10.1061/AJRUA6.0000909

Lu, X., Yu, H., Ying, M., Zhao, B., Zhang, S., Lin, L., Bai, L., Wan, R., 2021. Western North Pacific Tropical Cyclone Database Created by the China Meteorological Administration. Adv. Atmospheric Sci. 38, 690–699. https://doi.org/10/gjn5qm

Lu, Q., Zhang, W. and Bagtzoglou, A.C., 2022. Physics-based reliability assessment of community-based power distribution system using synthetic hurricanes. ASCE-ASME Journal of Risk and Uncertainty in Engineering Systems, Part A: Civil Engineering, 8(1), p.04021088. https://doi.org/10.1061/AJRUA6.0001205

Montes-Iturrizaga, R. and Heredia-Zavoni, E., 2016. Multivariate environmental contours using C-vine copulas. Ocean engineering, 118, 68-82. https://doi.org/10.1016/j.oceaneng.2016.03.011

Nelsen, R.B., 2006. An Introduction to Copulas (2nd ed.). Springer.

Johnson, R.A., Wehrly, T.E., 1978. Some angular-linear distributions and related regression-models. Journal of the American Statistical Association 73 (363), 602-606.

Russell, L.R., 1971. Probability Distributions for Hurricane Effects. J. Waterw. Harb. Coast. Eng. Div. 97, 139–154. https://doi.org/10/gnq54k

Song, Y.P., Basu, B., Zhang, Z.L., Sørensen, J.D., Li, J., Chen, J.B., 2021. Dynamic reliability analysis of a floating offshore wind turbine under wind-wave joint excitations via probability density evolution method. Renewable Energy 168, 991-1014.

Song, Y.P., Chen, J.B., Sørensen, J.D., Li, J., 2022. Multi-parameter full probabilistic modeling of long-term joint wind-wave actions using multi-source data and applications to fatigue analysis of floating offshore wind turbines. Ocean Engineering 247, 110676.

Thompson, E.F., Cardone, V.J., 1996. Practical modeling of hurricane surface wind fields. J. Waterw. Port Coast. Ocean Eng. 122, 195–205. https://doi.org/10.1061/(Asce)0733-950x(1996)122:4(195)

Tang, X.S., Li, D.Q., Zhou, C.B., Phoon, K.K., 2015. Copula-based approaches for evaluating slope reliability under incomplete probability information. Structural Safety 52, 90-99.

Tao, J.J., Chen, J.B., Ren, X.D., 2020. Copula-based quantification of probabilistic dependence configurations of material parameters in damage constitutive modeling of concrete. Journal of Structural Engineering 146 (9), 04020194.

Vickery, P.J., Skerlj, P.F., Twisdale, L.A., 2000. Simulation of Hurricane Risk in the U.S. Using Empirical Track Model. J. Struct. Eng. 126, 1222–1237. https://doi.org/10/crszwm

Vickery, P.J., Twisdale, L.A., 1995. Prediction of Hurricane Wind Speeds in the United States. J. Struct. Eng. 121, 1691–1699. https://doi.org/10/bd5357

Vickery, P.J., Wadhera, D., 2008. Statistical Models of Holland Pressure Profile Parameter and Radius to Maximum Winds of Hurricanes from Flight-Level Pressure and H*Wind Data. J. Appl. Meteorol. Climatol. 47, 2497–2517. https://doi.org/10.1175/2008jamc1837.1

Wang, H., Xu, M., Onyejuruwa, A., Wang, Y., Wen, S., Gao, A.E., Li, Y., 2019. Tropical cyclone damages in Mainland China over 2005–2016: losses analysis and implications. Environ. Dev. Sustain. 21, 3077–3092. https://doi.org/10.1007/s10668-019-00481-7

Willoughby, H.E., Rahn, M.E., 2004. Parametric Representation of the Primary Hurricane Vortex. Part I: Observations and Evaluation of the Holland (1980) Model. Mon. Weather Rev. 132, 3033–3048. https://doi.org/10/dkh4hk

Wu, F., Huang, G., Zhou, X., 2021. Enhanced Circular Subregion Method in Typhoon Hazard Analysis. J. Struct. Eng. 147, 06021003. https://doi.org/10.1061/(ASCE)ST.1943-541X.0003003

Xiao, Y.F., Duan, Z.D., Xiao, Y.Q., Ou, J.P., Chang, L., Li, Q.S., 2011. Typhoon wind hazard analysis for southeast China coastal regions. Struct. Saf. 33, 286–295. https://doi.org/10/dhttn6

Yuan, J., Wang, D., Wan, Q., Liu, C., 2007. A 28-year climatological analysis of size parameters for Northwestern Pacific tropical cyclones. Adv. Atmos. Sci. 24, 24-34. https://doi.org/10.1007/s00376-007-0024-y

Zhang, Y., Cao, S., Zhao, L., Cao, J., 2022. A case application of WRF-UCM models to the simulation of urban wind speed profiles in a typhoon. J. Wind Eng. Ind. Aerodyn. 220, 104874. https://doi.org/10/gnshmn